PAPER • OPEN ACCESS

$Li_4Ti_5O_{12}$ powders by spray-drying: influence of the solution concentration and particle size on the electrochemical properties

View the article online for updates and enhancements.

IOP ebooks™

Bringing you innovative digital publishing with leading voices to create your essential collection of books in STEM research.

Start exploring the collection - download the first chapter of every title for free.

$Li_4Ti_5O_{12}$ powders by spray-drying: influence of the solution concentration and particle size on the electrochemical properties

Claire Jamin, Thomas Jungers, Caroline Piffet, Abdelfattah Mahmoud, Rudi Cloots, Bénédicte Vertruyen, Frédéric Boschini

GREENMAT, CESAM Research Unit, B6a, University of Liège, Sart-Tilman, 4000 Liège, Belgium

[*]Corresponding author: phone: +32 4 366 3532; e-mail: frederic.boschini@ulg.ac.be

Abstract. The lithium battery electrode compound $Li_4Ti_5O_{12}$ was synthesized by calcination of precursor powders obtained through spray-drying of solutions prepared with titanium isopropoxide and lithium nitrate. X-ray diffraction and thermal analysis coupled to mass spectrometry show that single phase crystalline $Li_4Ti_5O_{12}$ particles can be obtained after calcination at 800 °C for 2 hours. Decreasing the solution concentration leads to smaller particle sizes but also to an unexpected decrease of the electrochemical capacity, probably related to the presence of residual Li_2TiO_3. On the contrary, the capacity of the $Li_4Ti_5O_{12}$ powder prepared with the high concentration solution can be increased from 150 mAh/g to 165 mAh/g (C/4 rate) by grinding. These results highlight the fact that smaller particles do not systematically display better performances for Li^+ intercalation/desintercalation and confirm the need for a comprehensive approach including parameters such as crystallinity, phase purity or agglomeration.

1. Introduction

As a negative electrode material in Li-ion batteries, lithium titanate $Li_4Ti_5O_{12}$ has a theoretical capacity of 175 mAh g^{-1} and a voltage plateau at ~1.55 V vs. Li^+/Li^0. Its excellent lithium intercalation/desintercalation reversibility is favored by the fact that there is almost no volume change during charge–discharge cycling [1,2]. Major advantages of $Li_4Ti_5O_{12}$ are low toxicity and low cost. Besides, $Li_4Ti_5O_{12}$ is the electrode material of choice when maximum safety is required, because Li^+ ions are intercalated at less negative potentials than in the usual carbon-based anodes [3,4], preventing lithium plating at high cycling rates [5]; decomposition of the electrolyte and formation of a passivation layer (solid-electrolyte interface – SEI) at the surface of the electrode are also prevented [6].

Many synthesis methods [7-13] have been investigated in the literature as alternatives to the standard solid state technique, targeting lower synthesis temperature, shorter reaction time and/or smaller particle size [14-16]. The spray-drying method [17] is particularly attractive because it has a good reproducibility and is easily upscalable to industrial level. Spray-drying takes place by atomization of a suspension or solution into small droplets injected in a drying chamber with a hot air flow. After solvent vaporization, the resulting solid particles are separated from the air flow and collected in a container. When applied to suspensions of pre-existing insoluble solid powders, the

spray drying technique is used to prepare dry granules of agglomerated powder. Several authors have used the spray drying of suspensions as an alternative to manually or mechanically mixing the reactants (typically a lithium salt and either anatase powder or in-situ generated TiO_2 colloidal particles) before solid state synthesis [18-23]. In the present work, we focus on spray drying of solutions, where excellent homogeneity is expected due to coprecipitation by solvent vaporization inside each individual droplet. This approach has been investigated by Yoshikiwa et al. [5] and Wu et al. [15,24,25] who studied the influence of the Li/Ti ratio and the temperature of heat treatment. Using the related technique of spray pyrolysis (where droplets are projected in a heated furnace), other authors [14] observed that modifications of the solution concentration affect the (micro)structural characteristics and the electrochemical performance of the $Li_4Ti_5O_{12}$ powders. It is therefore important to study how the solution concentration influences the synthesis of $Li_4Ti_5O_{12}$ by spray drying.

In the present work, $Li_4Ti_5O_{12}$ powders were prepared by spray-drying of solutions with concentrations ranging from 0.2 mol/l to 0.02 mol/l. The paper is divided in 3 parts, investigating respectively (1) the transformation of the as-sprayed powder into $Li_4Ti_5O_{12}$, (2) the influence of the solution concentration on the structure, microstructure and electrochemical capacity and (3) the influence of a further grinding step on the particle size and cycling performance.

2. Experimental

$Li_4Ti_5O_{12}$ powders were synthesized by heat treatment of precursor powders obtained by spray-drying of solutions with different concentrations: samples labelled LTO1, LTO2, LTO3 and LTO4 were obtained from solutions with titanium concentrations of 0.2, 0.1, 0.05 and 0.02 mol/l, respectively.

The solutions were prepared by dissolving 21.8 mmol titanium tetraisopropoxide (TTIP - Across, 99 % purity) and 17.4 mmol $LiNO_3$ (Aldrich, 99 % purity) in 6.5 ml isopropanol (VWR, HPLC 99 % purity) and 14 ml glacial acetic acid (Fisher, analytical grade); deionised water was subsequently added to the solutions under stirring to reach the final concentrations. Spray drying was performed in a lab-scale apparatus Büchi B-191 through a co-current atomizer (i.e., sprayed solution and drying air flow in the same direction) using a 0.7 mm nozzle. The inlet temperature was 120 °C with a liquid feed rate of 1.4 ml/min. The process was carried out in air, with atomizing pressure of 1 bar and a hot air flow rate of 700 normal l/h. The resulting powders were then calcined for 2 h in air at various temperatures from 200 °C to 800 °C.

Thermal analysis (thermogravimetry – TGA and differential scanning calorimetry – DSC) was performed with a Setaram TG-DSC111 system coupled and synchronized to a mass spectrometer (Pfeiffer Omnistar) for analysis of the evolved gases; powders were placed in alumina crucibles and heated in flowing air with a heating rate of 5 °C/min. X-ray diffraction patterns were recorded with a Siemens D5000 powder diffractometer (CuKα radiation, 15-65°2θ, 0.04° step size, 2.2 s/step). The TOPAS software was used for Rietveld refinement, using the fundamental parameters approach to model the instrumental contribution [26]. Fourier transform infrared (FTIR) spectroscopy was performed on powders dispersed in KBr disks. The powder morphology was characterized by scanning electron microscopy (Philips ESEM XL30 FEG). The particle size distribution was measured on isopropanol suspensions of calcined powders with a Mastersizer 2000 – Hydro 2000S apparatus (Malvern). Ball milling was performed at 200 rpm with a planetary crusher (Retsch PM 400/2), using a 7.5 wt% suspension in isopropanol. Electrochemical measurements were carried out with Swagelok two-electrode coin cells assembled in an argon glove box. 13 mm-diameter pellets were prepared by pressing, in a stainless steel grid, ca. 4 mg of a mixture of $Li_4Ti_5O_{12}$, acetylene black and polyvinylidene fluoride (PVDF) binder in 80:10:10 weight ratio. The counter electrode was metallic lithium, the current collectors were stainless steel and the separator between electrodes was a 25 μm monolayer polypropylene membrane (Celgard). The electrolyte was 1 mol/l $LiPF_6$ in ethylene carbonate:dimethylcarbonate (1/1 v/v). Galvanostatic discharge-charge curves were measured using a PAR 263A potentiostat, from 2 V to 1 V vs. Li^+/Li^0.

## 3.   Results and discussion

3.1.   From as-sprayed powder to $Li_4Ti_5O_{12}$

The powders obtained by spray-drying are amorphous and have to be calcined to induce crystallization. The formation of $Li_4Ti_5O_{12}$ from the LTO1 as-sprayed powder was studied by a combination of thermal analysis, FTIR spectroscopy and X-ray diffraction.

Thermogravimetry (TG) and differential scanning calorimetry (DSC) data were collected with a TG–DSC system coupled to a mass spectrometer (MS) for identification of the evolved gases. Figure 1 shows the TG curve, the DSC curve and the MS signals corresponding to m/z ratios of 18 (H_2O), 30 (NO) and 44 (CO_2). The thermal decomposition of the as-sprayed powder can be divided in three temperature ranges according to the inflexion points in the TG curve. Below 200 °C, the mass loss is due to endothermic release of water, corresponding to vaporization of loosely adsorbed water and decomposition of the –OH groups from the hydrolyzed titanium species. Between 200 °C and 400 °C, the exothermic progressive oxidation of organics into CO_2 and H_2O is accompanied by a first decomposition of nitrates. Finally, residual nitrates are decomposed between 450 °C and 550 °C, as confirmed by FTIR spectra (not shown) where the characteristic nitrate peak at 1380 cm^{-1} is still present in the sample heated to 400 °C and disappears after heating to 500 °C.
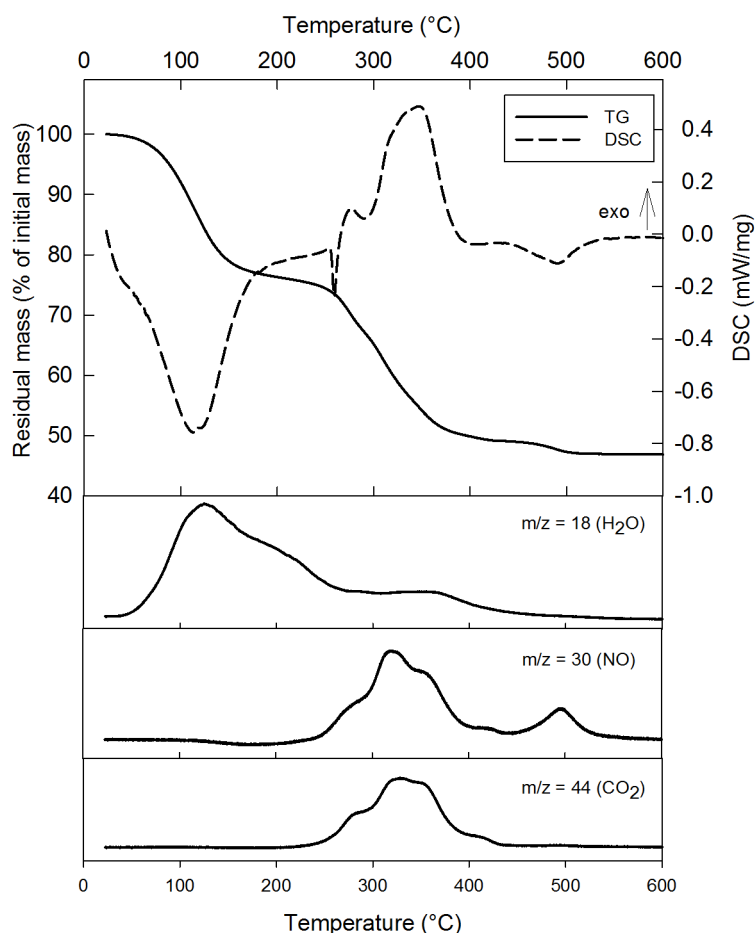
Figure 1. TGA, DSC and MS response for LTO1 spray-dryed powder, measured under air (5°C min^{-1}). The MS response related to H_2O, NO and CO_2 (m/z = 18, 30 and 44, respectively) is presented.

Figure 2 presents the XRD patterns of the LTO1 powders heated for 2 hours at temperatures from 200 °C to 800 °C. The onset of crystallization is observed after 2 hours at 300 °C with the presence of a weak diffraction peak corresponding to the (101) reflection of the anatase polymorph of TiO_2. After 2 hours at 500 °C, the reflections of the Li_2TiO_3 phase are clearly present, together with reflections from both the anatase and rutile polymorphs of TiO_2. The anatase-to-rutile transition is completed after 2 hours at 600 °C. After 2 hours at 700 °C, $Li_4Ti_5O_{12}$ becomes the major phase and increasing the temperature to 800 °C yields $Li_4Ti_5O_{12}$ without apparent secondary phase. These results show that $Li_4Ti_5O_{12}$ is formed by reaction between TiO_2 and Li_2TiO_3. Crystallization of Li_2TiO_3 and TiO_2 intermediate phases is commonly observed when $Li_4Ti_5O_{12}$ is synthesized with titanium alkoxide reactants because TiO_2 nuclei are easily formed by condensation of the hydrolyzed titanium species [5].
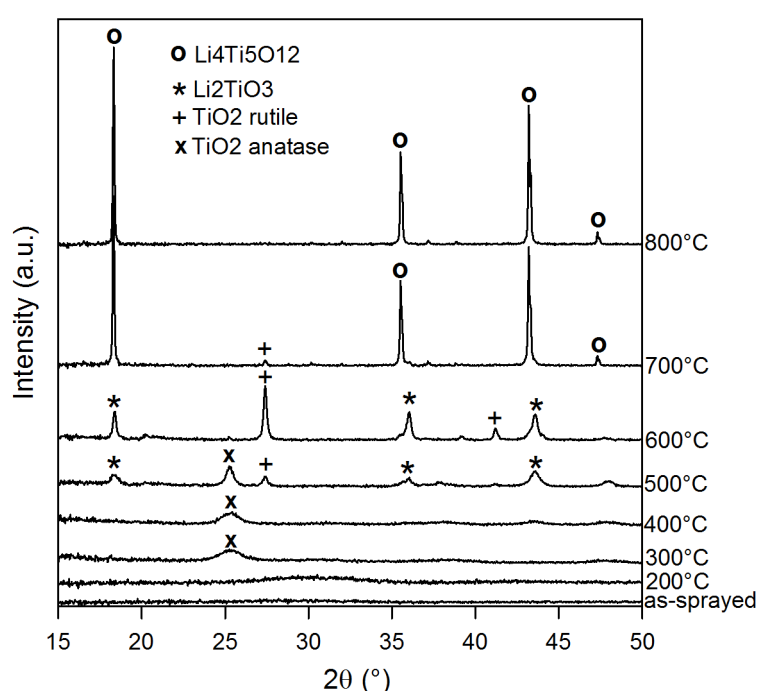

Figure 2. XRD patterns of LTO1 heated for 2 hours at temperatures from 200 °C to 800 °C.

3.2. Influence of the solution concentration

Figure 3 shows how a decrease of the solution concentration from 0.2 mol/l (LTO1) to 0.1 mol/l (LTO2), 0.05 mol/l (LTO3) or 0.02 mol/l (LTO4) affects the crystallinity and microstructure of the powders heated at 800 °C for 2 hours. The XRD patterns in the left column of figure 3 indicate that the $Li_4Ti_5O_{12}$ main phase is contaminated by a residual Li_2TiO_3 phase in the case of the powders prepared using the two most dilute solutions. The Li_2TiO_3 contents estimated by Rietveld refinement are 3 wt% and 15 wt% in the LTO3 and LTO4 powders, respectively. The absence of TiO_2 reflections (not shown) suggests that the $Li_4Ti_5O_{12}$ and Li_2TiO_3 phases might be slightly off-stoichiometric ($Li_{4-x}Ti_5O_{12-x/2}$ and $Li_{2-y}TiO_{3-y/2}$), due to incomplete diffusion of lithium from Li_2TiO_3 into TiO_2.

Scanning electron micrographs displaying the microstructures of the calcined powders are shown in the middle column of figure 3. In all cases, the solidified crusts of the droplets have shapes very different from spherical hollow spheres, indicating that buckling of the droplets occurred during spray drying; such a behavior is frequently reported in the literature [17,27] and there have been many attempts to model the mechanical instabilities in drying droplets [17,28]. The SEM micrographs also suggest some agglomeration of the dried droplets. In order to probe the strength of these agglomerates,

4th Euro-Mediterranean Conference on Materials and Renewable Energies   IOP Publishing
(EMCMRE-4), May, 8-11, 2017, Marrakech-Morocco

IOP Conf. Series: Journal of Physics: Conf. Series **1081** (2018) 012001   doi:10.1088/1742-6596/1081/1/012001

the particle size distributions were measured before and after ultrasonication and are shown in the right column of figure 3. The agglomerates are characterized by $d_{0.5}$ values of about 20 μm in all powders. Ultrasonication shifts the $d_{0.5}$ down to values between 3.5 and 5.5 μm except for the LTO4 powder with a $d_{0.5}$ that does not go below 8 μm. Comparing these values with the apparent sizes in the SEM micrographs, these results suggest the formation of stronger agglomerates in the case of powders synthesized with lower concentrations of precursor solutions.
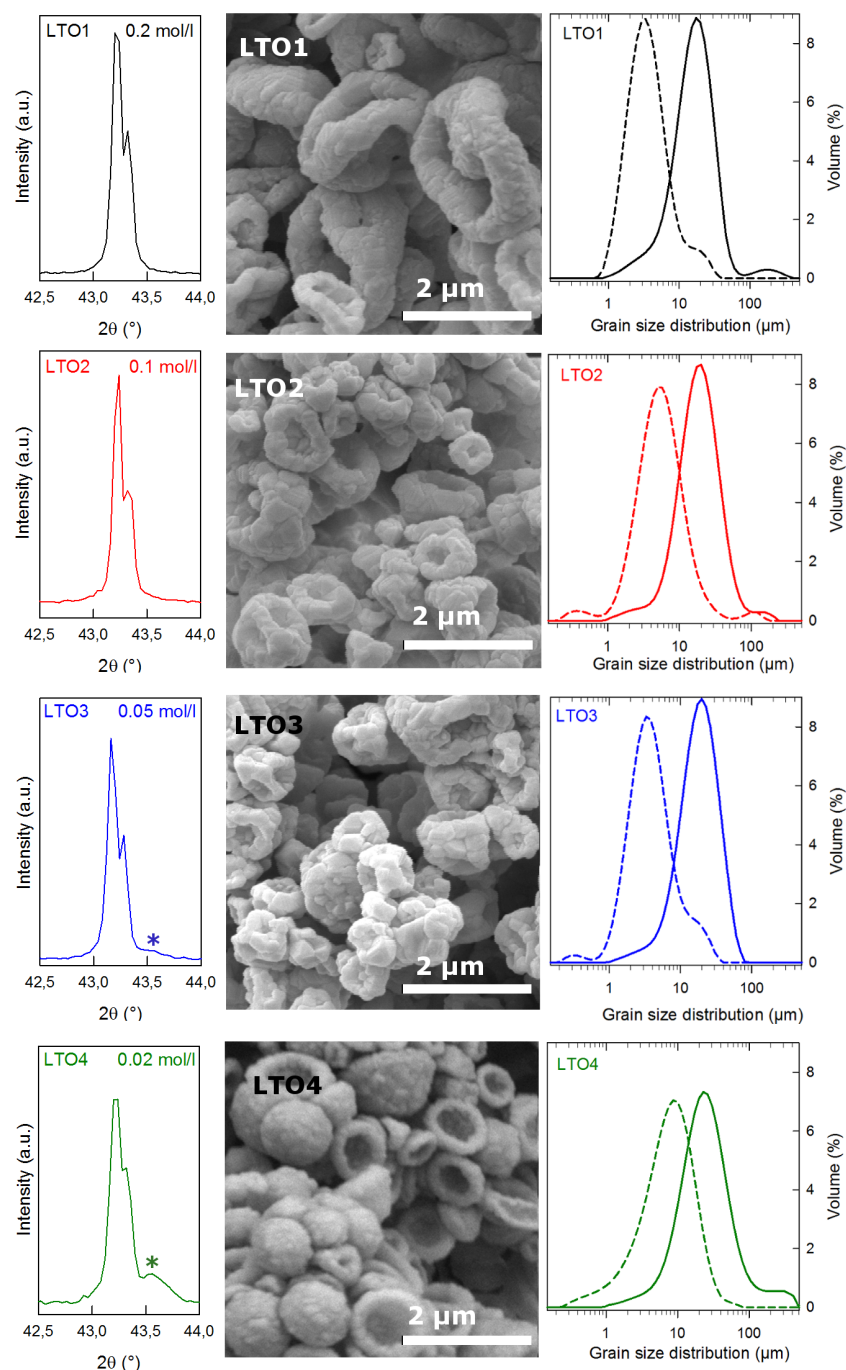
Figure 3. Comparison of powders heated at 800°C for 2 hours: (left) 42.5–44.0° 2θ range in the XRD pattern with Li_2TiO_3 secondary phase highlighted by an asterisk; (middle) scanning electron micrographs; (right) particle size distributions.

The electrochemical properties of the powders heated at 800 °C for 2 h were characterized by galvanostatic cycling at C/4 rate. Figure 4 presents the second discharge curves with capacity values quoted per gram of powder. The best capacities (~ 150 mAh g^{-1}) are obtained for the LTO1 and LTO2 powders. The LTO3 and LTO4 powders have lower capacities, 110 and 103 mAh g^{-1} respectively. These two powders contain residual Li_2TiO_3 phase, which is electrochemically inert [29,30]. However, the decrease in capacity is by ~30 % while the Li_2TiO_3 phase represents max. 15 wt%. This suggests that the grain size distribution and especially the formation of agglomerates contributes to the reduction of the electrochemical capacity, so that decreasing the solution concentration in the hope of obtaining smaller particles does not lead to the expected improvement of the electrochemical performance. In summary, the best results were obtained for the powders prepared from the solutions with the highest concentrations. The last section of this paper investigates whether a further improvement can be obtained by grinding the powder.
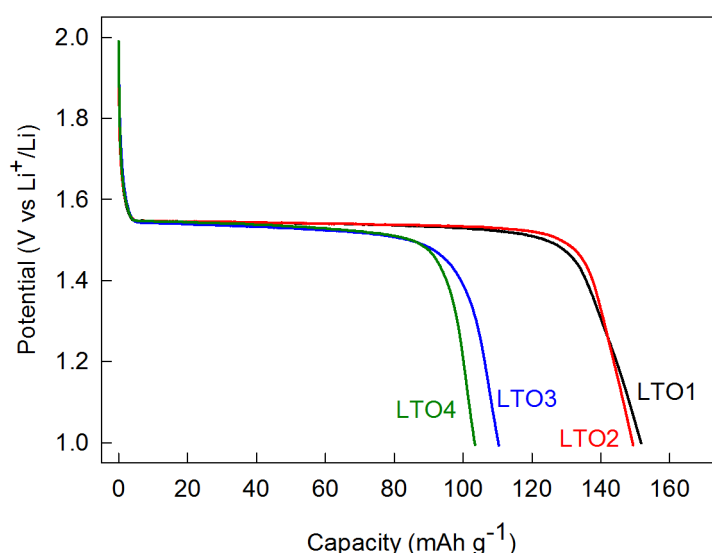
Figure 4. Discharge curves at C/4 rate in the voltage range 1.0–2.0 V.

3.3. Influence of grinding

To investigate the effect of grain size on the electrochemical properties, the LTO1 powder was ground for up to 4 hours. Figure 5 shows the SEM micrographs of the powder before grinding and after 30 min, 1 h or 4 h grinding. After 30 minutes or 1 hour of grinding, the majority of the dried droplets were broken into smaller pieces made up of joined primary particles. 4 hours of grinding leads to further reduction of the size of the primary particles into nanoparticles. The bottom of figure 5 presents the second discharge curves at C/4 rate for the LTO1 powder before and after grinding. The capacity tends to increase with decreasing particle size, from 152 mAh g^{-1} (before grinding) to 165 mAh g^{-1} (after 4 h of grinding). The shape of the curve before and after the plateau also changes with grinding, especially for the powder ground during 4 hours. This may be related to the partial amorphisation detected as a decrease of the XRD signal intensity, with the area under the main $Li_4Ti_5O_{12}$ reflection decreasing by 15 % after 1 h and 45 % after 4 h (not shown). Borghols and al. have suggested that this voltage profile, typical for nanoparticles, might be the consequence of strain and/or interface energy, which has relatively more impact in smaller particles [31].

Figure 6 compares the electrochemical capacity retention of the LTO1 unground powder with the LTO1 powder ground for 4 hours, assessed by measuring 30 galvanostatic charge/discharge cycles at C/4 rate and 10 galvanostatic charge/discharge cycles at C, 4C, 10C and C/4 rates. The behavior of both powders is qualitatively similar, with a good capacity retention at C/4 rate after the first few

cycles and the usual decrease in capacity at faster cycling speeds (C, 4C, 10C). Quantitatively, the capacities are systematically higher in the case of the ground powder, due to the larger surface area resulting from the smaller grain size.
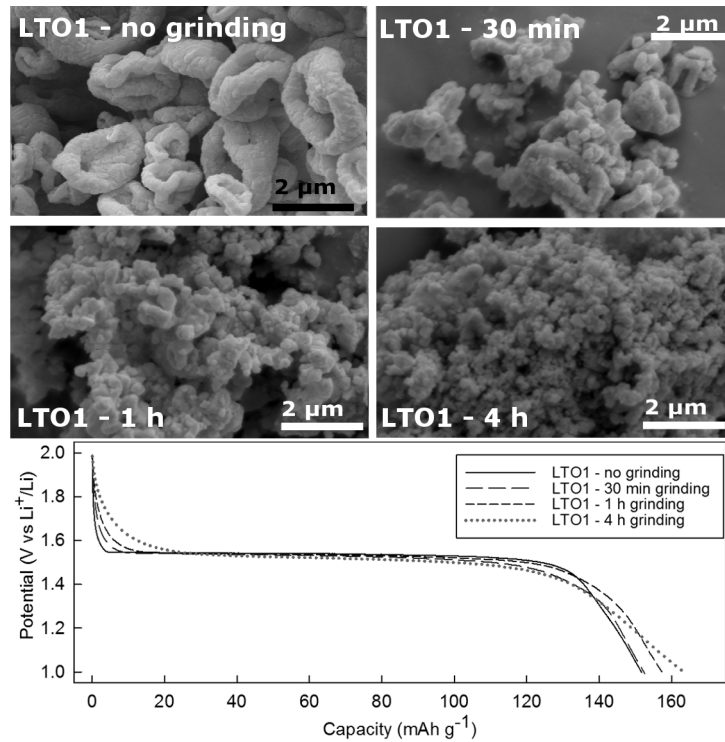
Figure 5. SEM micrographs and discharge curves at C/4 rate of the LTO1 powder before grinding and after 30 min, 1 h or 4 h grinding.
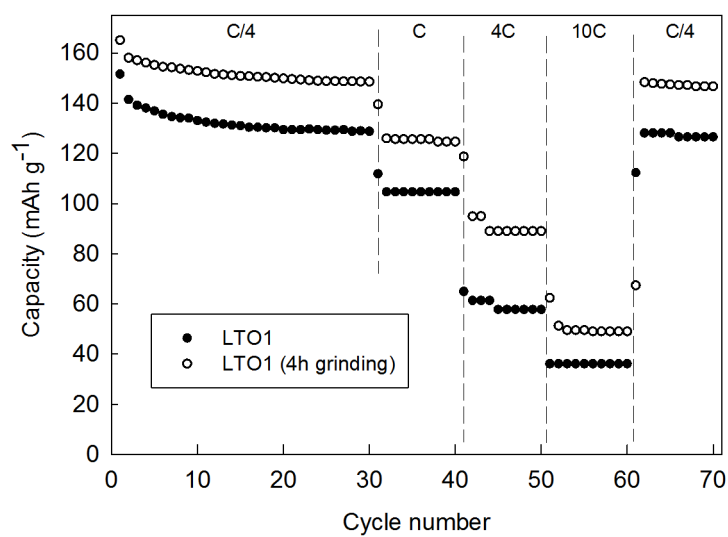
Figure 6. Rate capability of LTO1 without grinding and after 4 h grinding.

4. Conclusion

$Li_4Ti_5O_{12}$ was synthesized by spray drying of solutions with several concentrations. The $Li_4Ti_5O_{12}$ phase is formed at 700 °C and above by reaction between TiO_2 and Li_2TiO_3 intermediary phases in the precursor powders. The morphology and agglomeration of the particles after 2 h at 800 °C varies according to concentration of the precursor solution. Decreasing the solution concentration leads to smaller particles but residual Li_2TiO_3 is present and the electrochemical capacity tends to decrease. The best electrochemical performance is displayed by the powder prepared from the high concentration solution and can be further improved by grinding to reach 165 mAh/g at C/4 rate.

5. References

[1]   Yi T F, Jiang L J, Shu J, Yue C-B, Zhu R S and Qiao H B 2010 *J. Phys. Chem. Solids* **71** 1236–42
[2]   Ohzuku T, Ueda A and Kouguchi M 1995 *Electrochem. Soc.* **142** 1431–5
[3]   Hayner C M, Zhao X and Kung H H 2012 *Annu. Rev. Chem. Biomol. Eng.* **3** 445–71
[4]   Gao J, Jiang C and Wan C 2010 *Ionics* **16** 417–24
[5]   Yoshikawa D, Kadoma Y, Kim J M, Ui K, Kumagai N, Kitamura N and Idemoto Y 2010 *Electrochem. Acta* **55** 1872–9
[6]   Zaghib K, Dontigny M, Guerfi A, Charest P, Rodrigues I, Mauger A and Julien C M 2011 *J. Power Sources* **196** 3949–54
[7]   Prakash A S, Manikandan P, Ramesha K, Sathiya M, Tarascon J M and Shukla A K 2010 *Chem. Mater.* **22** 2857–63
[8]   Jung H G, Kim J, Scrosatia B and Suna Y-K 2011 *J. Power Sources* **196** 7763–6
[9]   Li J, Jin Y L, Zhang X G and Yang H 2007 *Solid State Ionics* **178** 1590–4
[10]   Cheng L, Yan J, Zhu G N, Luo J-Y, Wang C X and Xia Y Y 2010 *J. Mater. Chem.* **20** 595–602
[11]   Ogihara T, Yamada M, Fujita A, Akao S and Myoujin K 2011 *Mater. Res. Bull.* **46** 796–800
[12]   Zou H, Zhang G and Shen P K 2010 *Mater. Res. Bull.* **45** 149–52
[13]   Jamin C, Traina K, Eskenazi D, Krins N, Cloots R, Vertruyen B and Boschini F 2013 *Mater. Res. Bull.* **48** 4641–6
[14]   Ju S H and Kang Y C 2009 *J. Power Sources* **189** 185-90
[15]   He Z, Wang Z, Wu F, Guo H, Li X and Xiong X 2012 *J. Alloys Compd.* **540** 39–45
[16]   Zhang Q, Peng W, Wang Z, Li X, Xiong X, Guo H, Wang Z and Wu F 2013 *Solid State Ionics* **236** 4016–22
[17]   Nandiyanto A B D and Okuyama K 2011 *Adv. Powder Technol.* **22** 1–19
[18]   Zhu G N, Liu H J, Zhuang J H, Wang C X, Wang Y G and Xia Y Y 2011 *Energy Environ. Sci.* **4** 4016–22
[19]   Han S W, Ryu J H, Jeong J and Yoon D H 2013 *J. Alloys Compd.* **570** 144–9
[20]   Hsieh C T, Chen I L, Jiang Y R and Lin J Y 2011 *Solid State Ionics* **201** 60–7
[21]   Hsiao K C, Liao S C and Chen J M 2008 *Electrochem. Acta* **53** 7242–7
[22]   Lee B and Yoon J R 2013 *Electron. Mater. Lett.* **9** 871–3
[23]   Han S W, Shin J W and Yoon D H 2012 *Ceram. Int.* **38** 6963–8
[24]   Wu F, Wang Z, Li X, Guo H, Yue P, Xiong X, He Z and Zhang Q 2012 *Electrochim. Acta* **78** 331–9
[25]   Wu F, Li X, Wang Z, Guo H, He Z, Zhang Q, Xiong X and Yue P 2012 *J. Power Sources* **202** 374–9
[26]   Cheary R W and Coelho A 1992 *J. Appl. Crystallogr.* **25** 109–21
[27]   Ståhl K, Claesson M, Killiehorn P, Lindén H and Bäcksöm K 2002 *Int. J. Pharm.* **233** 227–37
[28]   Tsapis N, Dufresne E R, Sinha S S, Riera C S, Hutchinson J W, Mahadevan L and Weitz D A 2005 *Phys. Rev. Lett.* **94** 018302
[29]   Soares A, Fraisse B, Morato F, Ionica-Bousquet C M and Monconduit L 2012 *J. Power Sources* **208** 440–6
[30]   Lu J, Peng Q, Wang W, Nan C, Li L and Li Y 2013 *J. Am. Chem. Soc.* **135** 1649–52

[31]   Borghols W J H, Wagemaker M, Lafont U, Kelder E M and Mulder F M 2009 *J. Am. Chem. Soc.* **131** 17786–92